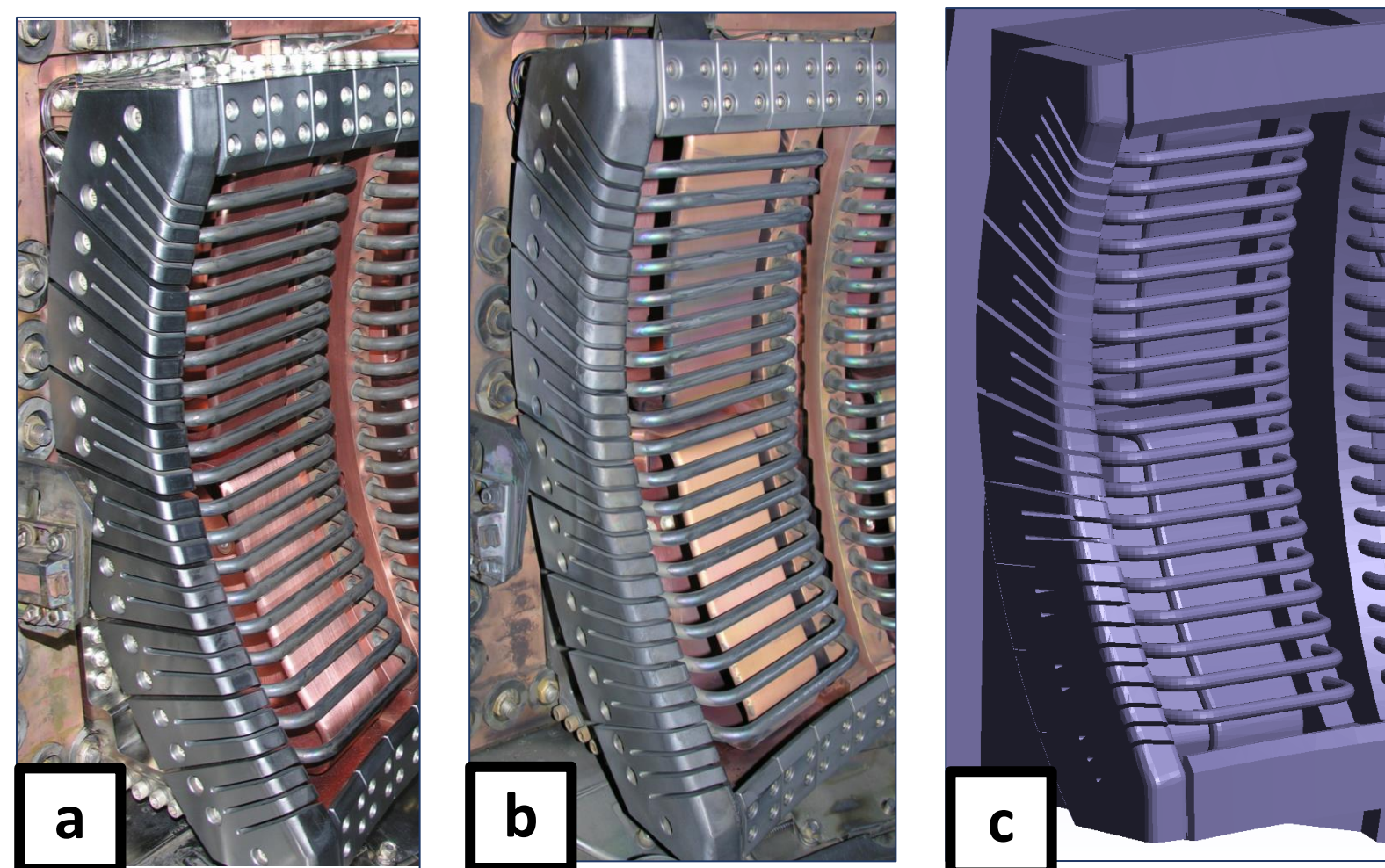


## Motivation

Impurities coming from the tokamak walls during ICRH antenna heating operation can contaminate the fusion plasma and cause:

- 1) Radiation power losses
- 2) Disruptions
- 3) Damage of the PFC

Understanding the physics of the plasma conditions in which the impurities get released has a crucial role in the healthy operation of a tokamak.



**Figure 1.** (a) ICRH antenna on C-Mod before plasma operations (b) ICRH antenna after plasma exposure; (c) CAD model [1].

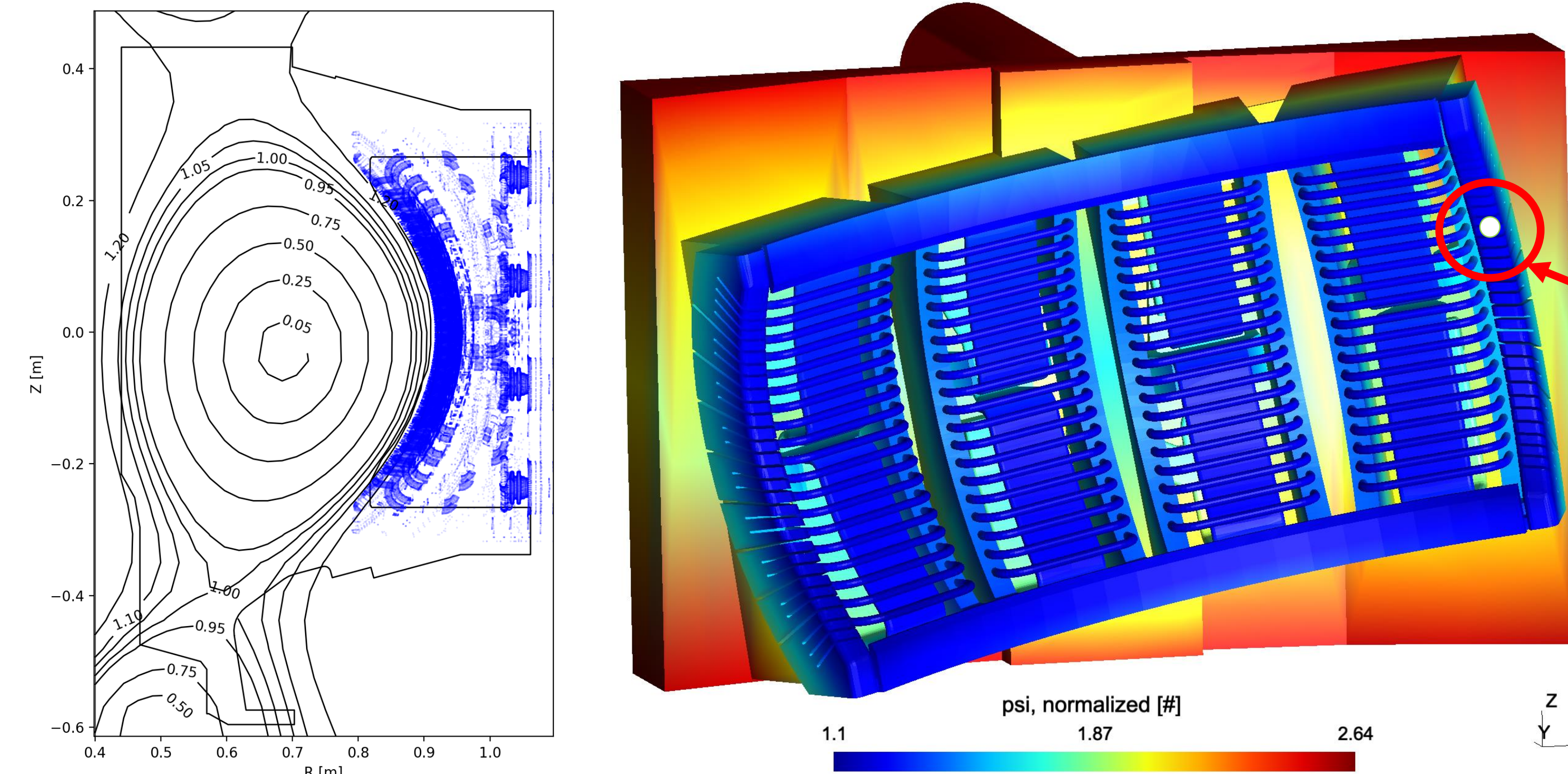
## Summary

- We calculated the nonlinear RF sheath boundary conditions using the STIX electromagnetic solver.
- Using the output from STIX code [2], we produced numerical simulations of the wall impurity flux produced during ICRH operations in Alcator C-Mod using the hPIC2 Particle-in-Cell code [3] and RustBCA ion-surface interaction code [4].
- We analyzed a deuterium plasma impacting on a Mo covered RF limiters surrounding the ICRH launcher at different levels of plasma contamination (Mo atomic concentration 0-5%).

## Conclusions

- 1) An increase of the impurity flux was determined from the hPIC2 code where the RF biasing caused a broadening of the ion energy distribution function (IED) due to the RF sheath.
- 2) Enhancement of Mo erosion flux as a function of the antenna strap phasing conditions also observed in the experiments.
- 3) **Next Steps:** Effects related to impurity charge distribution obtained from ionization balances are expected to modify the erosion fluxes significantly, and they will have to be considered.

## Magnetic Equilibrium and Antenna Location



## Step 1. hPIC2 – IEAD – Ion Energy Angle Distributions

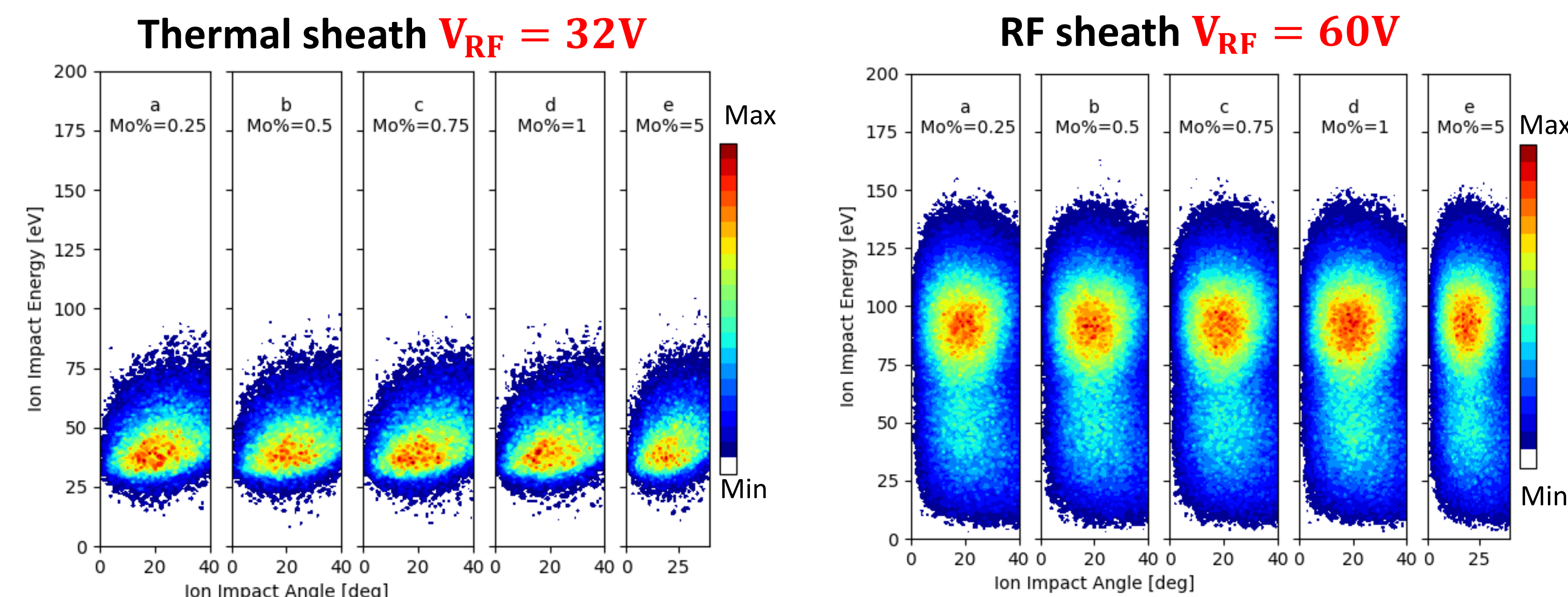


**Figure 2.** IEADs with one-peak energy structure of a thermal sheath centered at 37.5 eV and impact angles  $\theta \approx 20$

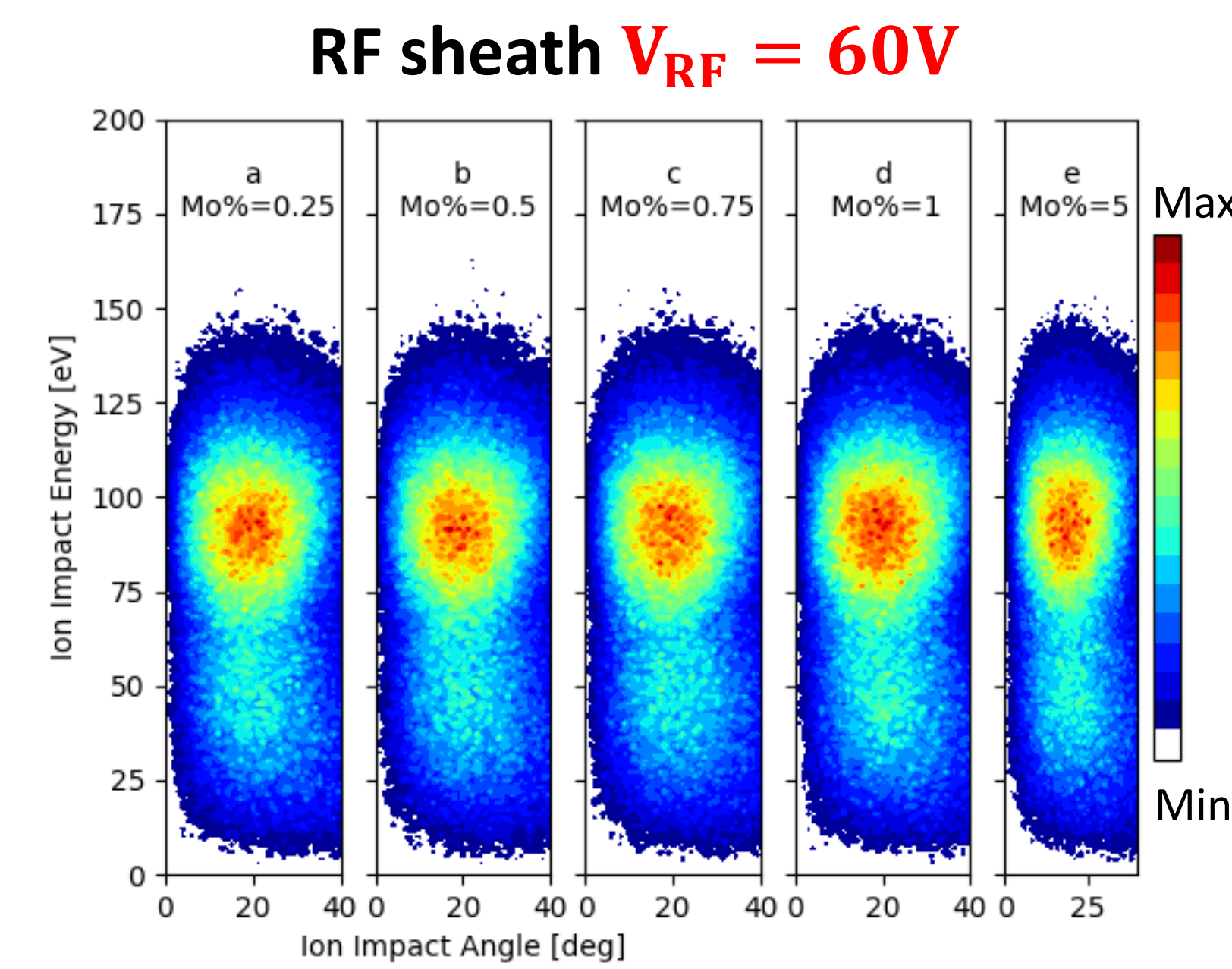


**Figure 3.** IEADs with typical two-peak energy structure of RF sheaths (RF peak at 90 eV). A high concentration of ions centered at impact angles  $\theta \approx 20$  is observed.

## Scan over Impurity Concentration

- D, main plasma species
- Two impurities assumed:
  - O as low-Z impurity
  - Mo as high-Z impurity

- Mo and O ranges are assumed in a range from 0.25-5.0% (atomic %)
- Furthermore, we assumed all impurities with unitary charge  $Z=1$

| Scenarios | D % (Z=1) | Mo % (Z=1) | O % (Z=1) |
|-----------|-----------|------------|-----------|
| a         | 98.75     | 0.25       | 1         |
| b         | 98.5      | 0.5        | 1         |
| c         | 98.25     | 0.75       | 1         |
| d         | 98        | 1          | 1         |
| e         | 94        | 5          | 1         |

Location on the region of interest from the STIX simulations (0.39, 0.84, 0.15) m

## Step 3. Erosion fluxes vs. Impurity Concentration

RF - OFF

Thermal sheath  $V_{RF} = 32V$ , IEAD peak at 37.5 eV

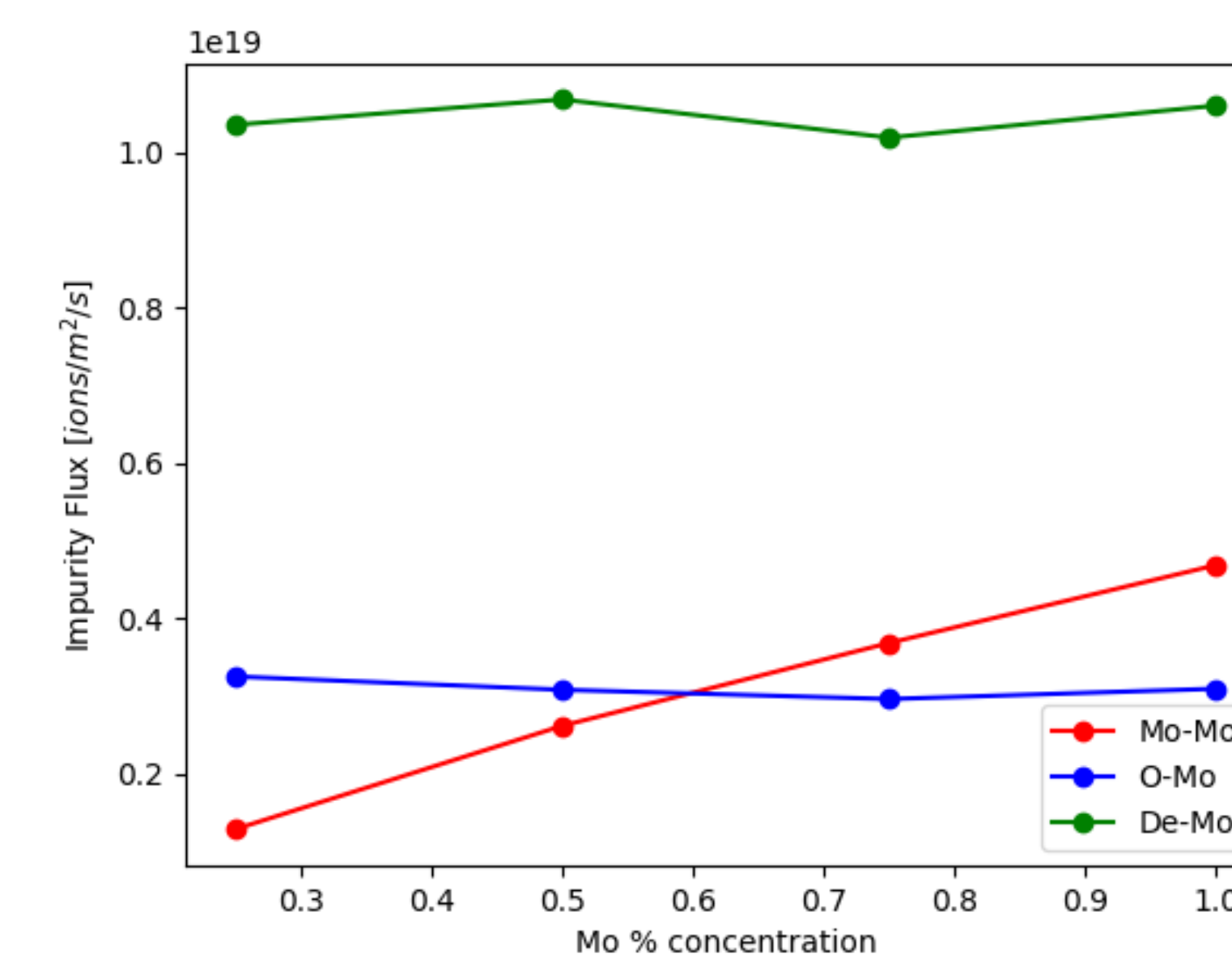


**Figure 4.** Impurity fluxes of Mo (red), O (blue) and De (green) in the thermal sheath formed at 32 V as a function of the Mo concentration. The impurity fluxes of low-z ions are non-negligible and higher than high-z impurities in the conditions of a thermal sheath.

RF - ON

RF sheath  $V_{RF} = 60V$ , IEAD RF peak at 90 eV

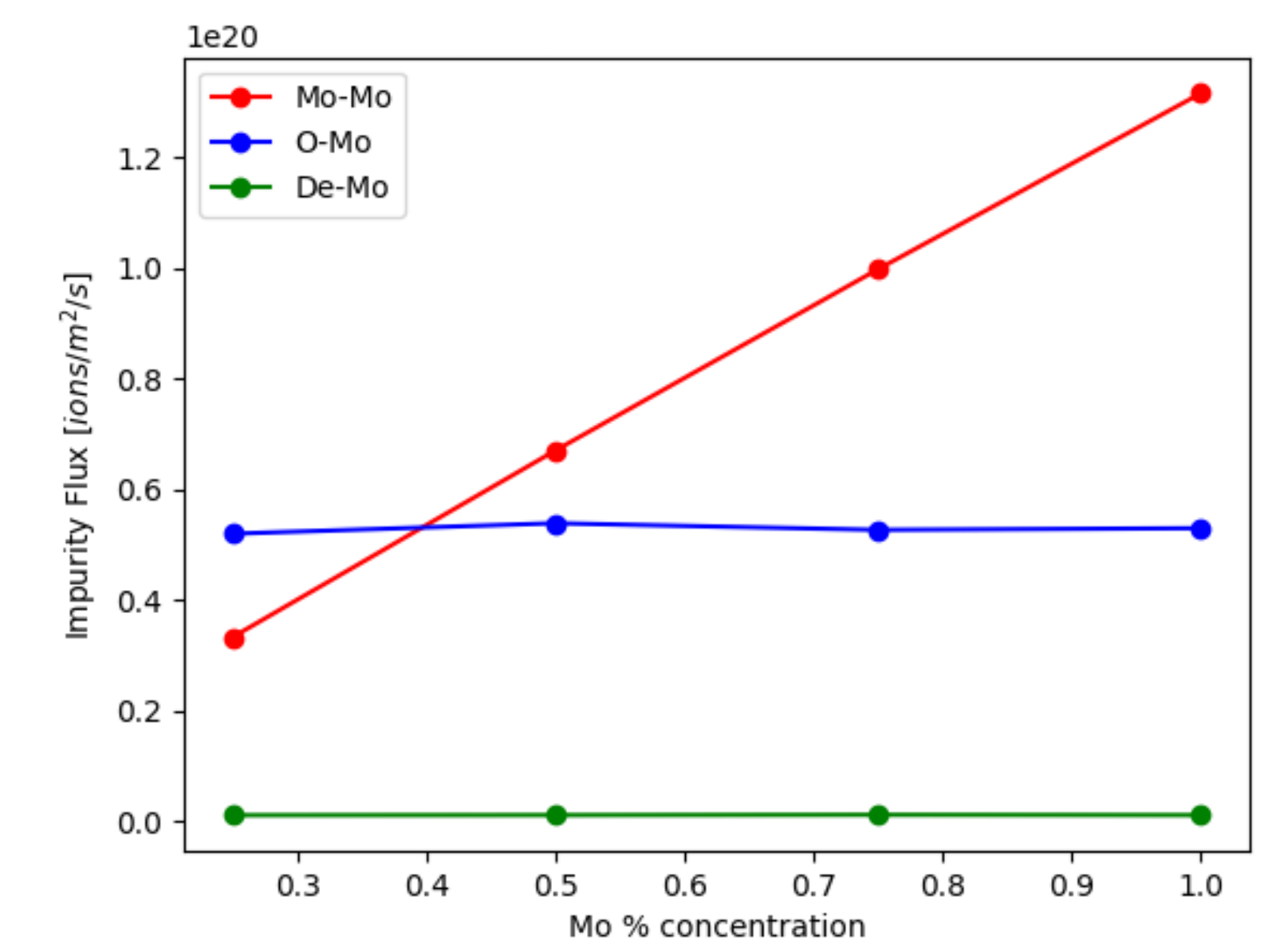


**Figure 5.** Impurity fluxes of Mo (red), O (blue) and De (green) as a function of the Mo concentration in an RF sheath formed at a rectified voltage of 60V. The impurities level is increased by an approximately a factor of 10 compared to the RF-OFF case.

## Workflow

STIX

Inputs:

$\Psi$ : Magnetic equilibrium data

Outputs:

$V_{RF}$ : rectified voltage

$B$ : magnetic field

$E$ : electric field

hPIC2

$$\frac{\partial f_s}{\partial t} + \vec{v} \cdot \nabla f_s + \frac{e}{m} (\vec{E} + \vec{v} \times \vec{B}) \cdot \nabla_{\vec{v}} f_s = 0$$

$$\frac{d^2 \phi}{dx^2} = -\frac{e}{\epsilon_0} (Z_s n_s - n_e)$$

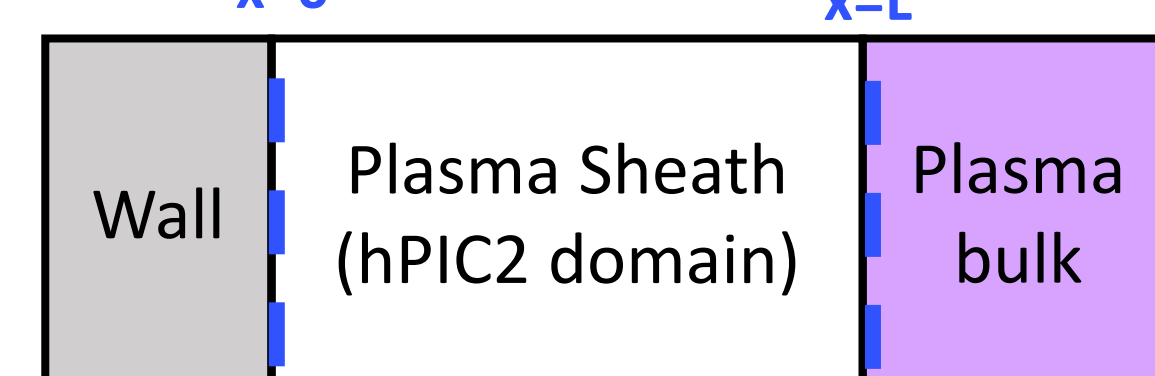
Where  $s = D, O, Mo$

- **Boundary conditions:**

$$\phi(x=0, t) = V_{RF} \sin(\omega t) - V_{DC}$$

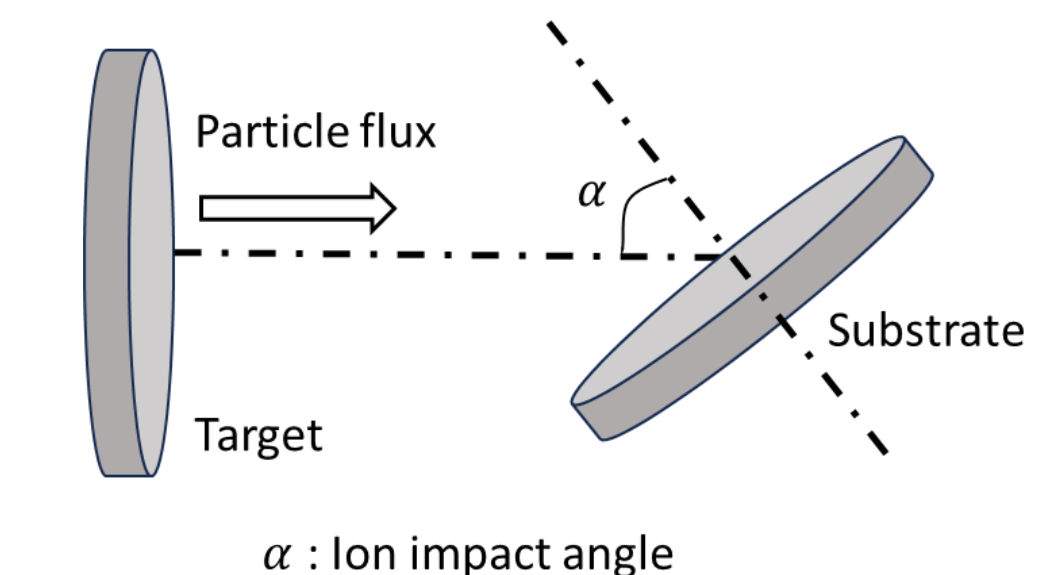
$$\frac{d\phi}{dx}(x=L, t) = 0$$

West boundary  $x=0$  East boundary  $x=L$



RustBCA

$$\bar{Y} = \iint Y(E_i, \theta_i) \hat{f}_i(E_i, \theta_i) dE_i d\theta_i$$



|                  |           |
|------------------|-----------|
| Ion impact angle | 20°       |
| Energy domain    | 10-200 eV |

Erosion flux

$$\Gamma_s = \Gamma_i \bar{Y}$$

## Step 2. RustBCA – Sputtering Yi

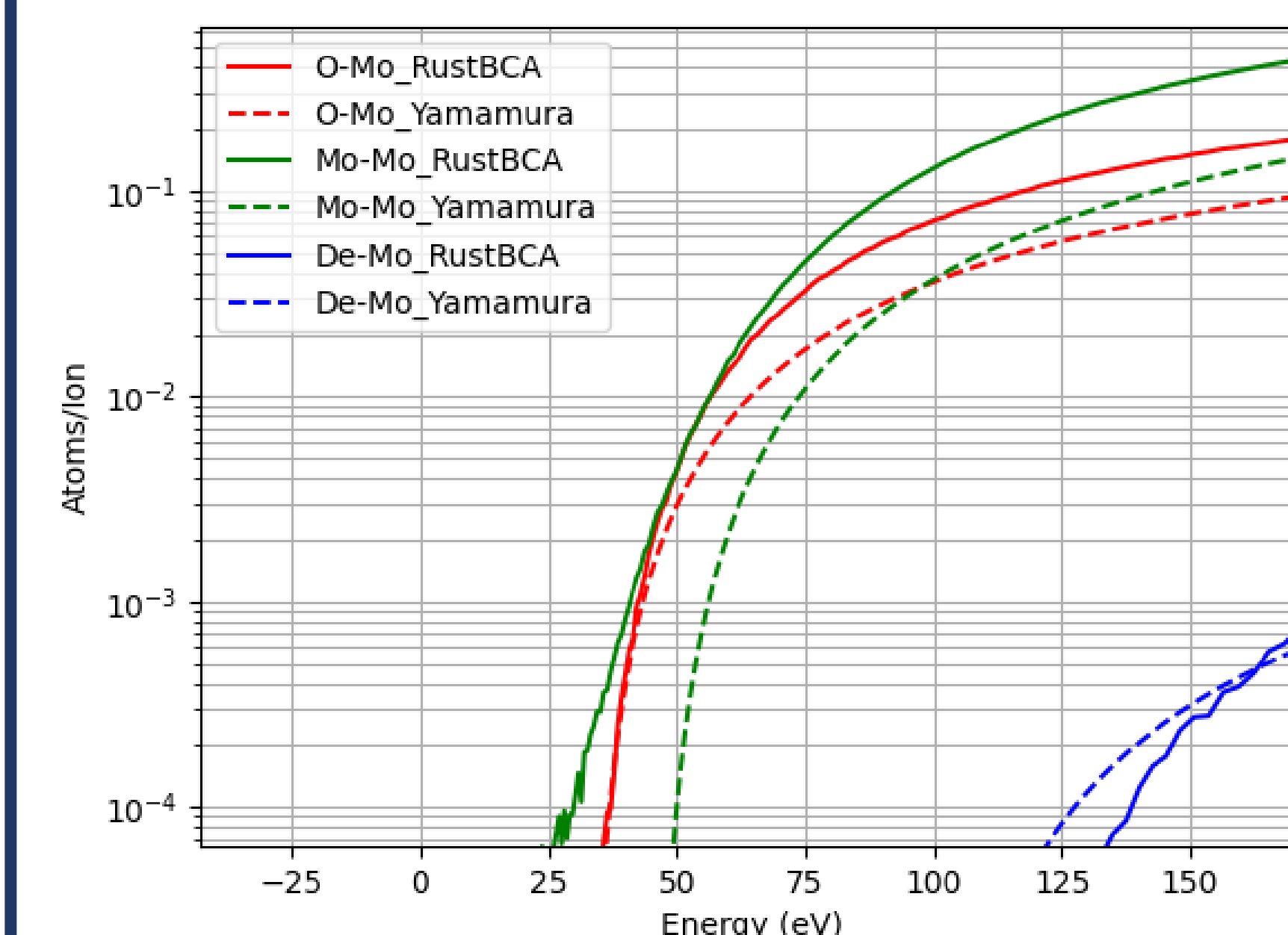


**Figure 6.** Maximum sputtering yield profiles of O-Mo, Mo-Mo and De-Mo calculated with RustBCA at 0 eV bulk binding energy (solid lines) in comparison to the empirical calculation using the Yamamura equation (dotted lines).

## References

1. PSFC-MIT. Available in: <https://www-internal.psfc.mit.edu/research/alcator/photos/NVESSEL/2015/Close%20up%20Survey%203-3-16/>
2. Migliore C. et al 2023 Development of impedance sheath boundary condition in Stix finite element RF code (arXiv:2306.12930)
3. L.T. Meredith, M. Rezazadeh, M.F. Huq, J. Drobny, V.V. Srinivasaragavan, O. Sahni, and D. Curreli. hpic2: A hardware-accelerated, hybrid particle-in-cell code for dynamic plasma-material interactions. Computer Physics Communications, 283:108569, 2023.
4. J.T. Drobny, D. Curreli. J. Open Sour. Softw., 6 (64) (2021), p. 3298, 10.21105/joss.03298

## Acknowledgement

This material is based upon work supported by the U.S. Department of Energy Office of Science, Office of Fusion Energy Sciences, Scientific Discovery through Advanced Computing, Center for Integrated Simulation of Fusion Relevant RF Actuators, Award Numbers DE-SC0018090-PO97564.